



ESTIMATING ICE ACCUMULATION ON SURFACE STRUCTURES

By

William R. Schaub, Jr.



JUNE 1995



APPROVED FOR PUBLIC RELEASE;
DISTRIBUTION IS UNLIMITED.

USAF Environmental Technical Applications Center
859 Buchanan Street
Scott Air Force Base, Illinois 62225

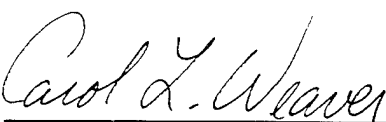
19951219 065

REVIEW AND APPROVAL STATEMENT

USAFETAC/TN—95/002, *Estimating Ice Accumulations on Surface Structures*, June 1995, has been reviewed and is approved for public release. There is no objection to unlimited distribution of this document to the public at large, or by the Defense Technical Information Center (DTIC) to the National Technical Information Service (NTIS).


JAMES H. DAVENPORT, Lt Col, USAF
Chief, Systems Division

FOR THE COMMANDER


CAROL L. WEAVER, PhD
Scientific and Technical Information
Program Manager
23 June 1995

REPORT DOCUMENTATION

2. Report Date: June 1995
3. Report Type: Technical Note
4. Title: Estimating Ice Accumulations on Surface Structures
6. Author: William R. Schaub, Jr.
7. Performing Organization Name and Address: USAF Environmental Technical Applications Center (USAFETAC/DOC), 859 Buchanan St., Scott AFB IL 62225-5116
8. Performing Organization Report Number: USAFETAC/TN—95/002
12. Distribution/Availability Statement: Approved for public release; distribution is unlimited.
13. Abstract: Proposes several methods for estimating ice accretion on surface structures based on estimates of several atmospheric variables. Also provides information on types of structural icing, ice accretion theory, and ice accretion computer modes.
14. Subject Terms: CLIMATOLOGY, ATMOSPHERIC ICING, ICING, STRUCTURAL ICING, ICE FORMATION, ICE ACCRETION, THEORY, FORECASTING, ICE FORMATION INDICATORS, ESTIMATES, STATISTICAL ANALYSIS, MODELS, MATHEMATICAL MODELS.
15. Number of Pages: 33
17. Security Classification of Report: Unclassified
18. Security Classification of this Page: Unclassified
19. Security Classification of Abstract: Unclassified
20. Limitation of Abstract: UL

Standard Form 298

PREFACE

This report documents the results of USAFETAC Project 930919, completed by USAFETAC's Simulation and Techniques Branch (USAFETAC/SYT). The project manager was Mr. William R. Schaub, Jr.

The customer was the Acquisition Meteorology Division of the Electronic Systems Center (ESC/WE) at Hanscom AFB, Massachusetts. The customer requested that USAFETAC improve its capability to estimate icing on structures, specifically: provide ice thicknesses for a 10-percent risk in a 10-year design life (95-year return period) for rime and glaze ice accumulations on both a 1/2-inch radius wire and a horizontal flat plate (as included on USAFETAC Form 3, Engineering Environmental Design Information, Part II). Algorithms are being coded for icing as this report is being published. The point of contact is Mr. Thomas Elio, USAFETAC/SYT, DSN 576-5412.

This report first provides background on the problem of estimating ice accumulation on surface structures. It also provides information on ice types, ice accretion theory, and computer models of ice accretion. Finally, methods are proposed for estimating ice accumulation on structures based on estimates of several atmospheric variables.

The author is grateful to Charles C. Ryerson at the U.S. Army Cold Regions Research and Engineering Laboratory for fruitful discussions on the structural icing problem. He is also grateful to Tsoi-Ching Yip at the Canadian Climate Centre who provided a paper on her evaluation of several icing models, and a paper on an operational

CONTENTS

1. INTRODUCTION	1
1.1 The Icing Problem	1
1.2 USAFETAC Support	1
1.3 Complicating Factors	1
1.4 USAFETAC'S Approach	2
1.5 Scope of this Report	4
2. BACKGROUND	5
2.1 Types of Atmospheric Icing	5
2.2 Factors Affecting Icing	5
2.3 Ice Shapes	7
2.4 Ice Accretion Theory	8
2.4.1 Forces on Droplets	8
2.4.2 Collection Efficiency	8
2.4.3 Equivalent Radial Thickness	9
2.5 Ice Accretion Models	9
2.5.1 Chaîne and Skeates Model	10
2.5.2 Makkonen Model	11
2.5.3 McComber and Govoni Model	12
3. METHODS FOR ESTIMATING ICING	13
3.1 General Considerations	13
3.2 Glaze Estimates from Freezing Precipitation	14
3.3 In-Cloud Rime and Glaze Estimates	14
3.3.1 Estimation of Input Variables	14
3.3.2 Application of McComber and Govoni Model	15
3.4 What to Expect	16
3.5 Variations of Ice Thickness on Tall Structures	18
3.6 Maximum Wind with Ice Loads	18
4. CONCLUSIONS	19
REFERENCES	20
GLOSSARY	22

Accession For	
NTIS GRA&I	<input checked="" type="checkbox"/>
DTIC TAB	<input type="checkbox"/>
Unannounced	<input type="checkbox"/>
Justification	
By	
Distribution/	
Availability Codes	
Dist	Avail and/or Special
A-1	

FIGURES

Figure 1. Section 16 of USAFETAC Form 3, Engineering Design Information (Part II)	1
Figure 2. Regions of similar glaze ice characteristics in the United States	2
Figure 3. Map of index of severity of freezing precipitation for Canada	3
Figure 4. Relationships of ice types with (a) droplet diameter, and (b) air temperature and wind speed	6
Figure 5. Shape of soft rime accretions on an object oriented normal to the wind flow	7
Figure 6. Same as Figure 5 except for hard rime	7
Figure 7. Same as Figure 5 except for side view only	7
Figure 8. Collection (catch) efficiency of a cylinder	8
Figure 9. Variations in shapes of ice accumulations on wires	9
Figure 10. Correction factors (K) for various wire diameters and temperature ranges	10
Figure 11. Results of numerical simulation of ice accretion on a 1-cm diameter wire	11
Figure 12. Time-evolution of the freezing fraction (n) and the collection efficiency (E)	11
Figure 13. Extreme value analysis of annual maximum ice thickness (cm) for Monte Cimone, Italy	17
Figure 14. Variation of average diameters of glaze and hard rime accumulations with height above ground	18

TABLES

Table 1. Return periods for specified calculated risk and design life	2
Table 2. Ice thickness, estimated to the nearest 0.1 cm, combined with wind gusts greater than 40 knots in the most severe location in each region shown in Figure 2.	3
Table 3. Characteristics of glaze and rime ice	5
Table 4. Annual maximum ice thickness (cm) for Monte Cimone, Italy	16

Chapter 1

INTRODUCTION

1.1 The Icing Problem. Atmospheric icing of objects on the earth's surface often results in widespread damage. An example is the structural failure of power transmission lines and towers due to the weight of accumulated ice. The ice loads are usually followed by strong winds that add to the stress on the structures. Engineers need estimates of expected icing for use in designing structures such as communications towers to withstand the icing and wind conditions that may occur during the lifetime of the structures.

1.2 USAFETAC Support. Since the early 1970s, the Engineering Meteorology Section of the USAF Environmental Technical Applications Center (USAFETAC) has provided icing and wind information for structural design. The ice information

is part of a comprehensive, site-specific climatology for the desired location.

As shown in Figure 1, the Ice Information section of USAETAC Form 3 provides estimates of rime and glaze ice expected on a 1/2-inch radius wire and a flat plate. The wire is assumed to be perpendicular to the wind flow, while the plate lies horizontal in the wind flow. Also included is an estimate of the maximum wind expected with the ice in place. The 10-percent risk in a 10-year design life states that the information is for a structure designed to last 10 years, during which time the values given only have a 10-percent probability of being equaled or exceeded. Those risk and design life criteria define ice amounts expected with a storm that occurs on an average of once every 95 years. See Table 1, next page, from Air Weather Service (1977).

16. ICE INFORMATION: Ten percent risk in a 10 year design life.		
BASED ON A 0.5 INCH RADIUS WIRE	RIME ICE	
	GLAZE ICE	
BASED ON A HORIZONTAL FLAT PLATE	RIME ICE	
	GLAZE ICE	
MAXIMUM WIND WITH ICE LOADS (KNOTS)		

Figure 1. Section 16 of USAFETAC Form 3, Engineering Environmental Design Information (Part II).

1.3 Complicating Factors. Observations of rime and glaze icing are not made routinely. Even where observations *have* been made, the instrumentation and techniques have not been standardized. Remote hilly and mountainous regions (favorite places to site communications towers, radars, and the like) are far removed from regularly reporting weather stations. Icing observations are extremely limited except where research has been conducted. Due to the limited icing data, climatologists are forced to estimate icing from

atmospheric variables that *are* regularly observed. Even the observed variables themselves must often be estimated from the closest reporting station. Strictly speaking, an extreme value analysis is required (Air Weather Service, 1977) to obtain icing values for a 95-year return period or any other return periods. Input values for the analysis are maximum annual ice accumulations for at least 2 years, but preferably 5 years or more (Ryerson, 1987).

TABLE 1. Return Periods for specified calculated risks and design life (adapted from Air Weather Service 1977).

Calculated Risk [f(x)n]	Design Life in Years (n)*											
	1	2	3	4	5	10	15	20	25	30	35	40
0.01	100	199	299	398	498	996	1493	1991	2488	2986	3483	3981
0.02	50	99	149	198	248	495	743	990	1238	1485	1733	1980
0.03	33	66	99	132	165	329	493	657	821	985	1150	1314
0.04	25	49	74	98	123	245	368	490	613	735	858	980
0.05	20	39	59	78	98	195	293	390	488	585	683	780
0.10	10	19	29	38	48	95	143	190	238	285	333	380
0.15	7	13	19	25	31	62	93	124	154	185	216	247
0.20	5	9	14	18	23	45	68	90	113	135	157	180
0.25	4	7	11	14	18	35	53	70	87	105	122	140
0.30	3	6	9	12	15	29	43	57	71	85	99	113
0.35	3	5	7	10	12	24	35	47	59	70	82	93
0.40	3	4	6	8	10	20	30	40	49	59	69	79
0.45	2	4	6	7	9	17	26	34	42	51	59	67
0.50	2	3	5	6	8	15	22	29	37	44	51	58

1.4 USAFETAC'S Approach. Due to icing data limitations, USAFETAC has relied heavily on reports of major icing events, case studies, and regional information on icing to make ice thickness estimates. Reports of extreme icing events are usually not received until damage has occurred, as in the case studied by Schaub (1981). As stated by Boyd (1970),

“Observations of both thickness and density (of ice) are scarce, and the long records needed for statistical analyses are lacking. It will be necessary, therefore, to use whatever thickness reports can be found and assume a maximum density (when estimating ice thickness) to be on the safe side.”

Regional studies have been useful in making icing estimates. As an example, Tattelman and Gringorten (1973) built on the work of Bennett (1959) to estimate glaze ice thicknesses combined with wind gusts

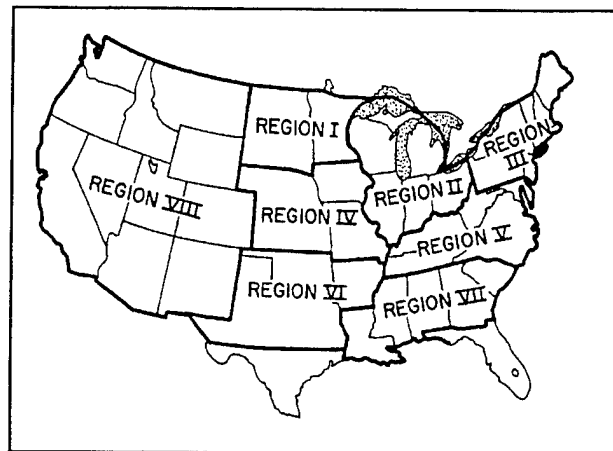


Figure 2. Regions of similar glaze ice characteristics in the United States (from Tattelman and Gringorten 1973).

greater than 40 knots for seven regions of the United States (Figure 2).

Region	Return Period (Years)		
	25	50	100
I	2.5	5	6.5
II	3.7	5	6.5
III	2.6	5	6.6
IV	<2.5	3.5	5.6
V	<2.5	<2.5	3.6
VI	<2.5	3	4.5
VII	<2.5	2.5	4.1

TABLE 2. Ice thickness, estimated to the nearest 0.1 cm, combined with wind gusts greater than 40 knots in the most severe location in each region shown in Figure 2 (based on data for 1919-1969 from Tattelman and Gringorten, 1973).

The extreme values of glaze ice thickness combined with wind gusts greater than 40 knots are shown in Table 2 for various return periods. Boyd (1970) used icing reports from telephone and electric companies in Canada during 1965-70 to determine that the greatest and most frequent thicknesses of ice on structures occurred in eastern Newfoundland. He also used data from McKay and Thompson (1969) for 1957-66 to produce a map of index of severity of freezing precipitation in Canada (Figure 3).

As another example, USAFETAC used a study by Chaine and Skeates (1974) that gives extreme value analyses of glaze ice thicknesses and winds out to a 40-year return period for 148 stations across Canada based on 9 to 15 years of data. Examples of rime icing studies are more limited because rime typically occurs on isolated hills and in mountains. An exception is Mount Washington, New Hampshire, where icing studies have been conducted since the late 1930s (Putnam, 1991).

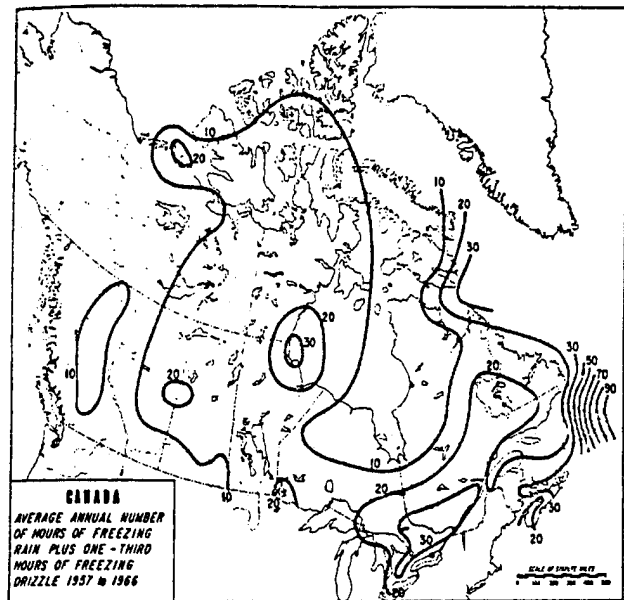


Figure 3. Map of index of severity of freezing precipitation for Canada (from Boyd, 1970).

CHAPTER 1

1.5 Scope of this Report. The original scope of this report was to review the scientific literature and summarize the state of knowledge concerning structural icing. Because the literature on structural icing is so extensive, a thorough review of all aspects of structural icing was not possible. Instead, this report

focuses on providing background information on ice types, ice accretion theory, and computer models of ice accretion in Section 2. The third chapter provides recommended procedures for estimating ice accretion.

Chapter 2

BACKGROUND

2.1 Types of Atmospheric Icing. There are three types of atmospheric icing: *glaze*, *hard rime*, and *soft rime*. The special case of icing on structures due to wet snow buildup is not covered in this report.

Glaze accumulates on surface objects due to freezing precipitation or from supercooled water droplets in fog or cloud, carried in the wind flow, that impinge on objects whose surface temperatures are at or a few degrees below freezing. Rime ice forms only rarely as a result of freezing precipitation; it forms most often from supercooled droplets contracting objects that are below freezing. Rime occurs mostly in hilly and mountainous areas that are often enshrouded by clouds. Table 3, from Minsk (1977), describes the characteristic appearance, density, and conditions of formation for each of the three icing types.

2.2 Factors Affecting Icing. Ice type is determined by air temperature, wind speed, supercooled droplet diameter, and liquid water content. The relationships of ice types with droplet diameter, air temperature, and wind speed are shown in Figure 4, next page.

Glaze is favored by a relatively large droplet diameter, air temperature in a narrow range at and just below freezing, and relatively high wind speeds. Conversely, rime forms when droplet diameters are relatively small, and when air temperature and wind speed are low. The liquid water content is a contributing factor to ice type because it varies according to median-volume droplet diameter, as shown in Makkonen (1984a).

Table 3. Types and characteristics of atmospheric icing (from Minsk, 1977).

Type of ice	Appearance	Density (g/cm ³)	Conditions of formation
Glaze	A hard, well-bonded, generally clear homogeneous ice	0.7-0.9	Supercooled water droplets at a temperature close to freezing (0 to -3° C) and wind speeds of 1-20 m/s
Hard rime	A hard, granular white or translucent ice growing into the direction of the wind	0.1-0.6	Supercooled water droplets at a temperature of -3 to -8° C, wind speeds generally 5-10 m/s
Soft rime	A white, opaque, granular ice with delicate structure only loosely bonded, growing into the direction of the wind	0.01-0.08	Supercooled water droplets at a temperature of -5 to -25° C, and low wind speed (1-5 m/s)

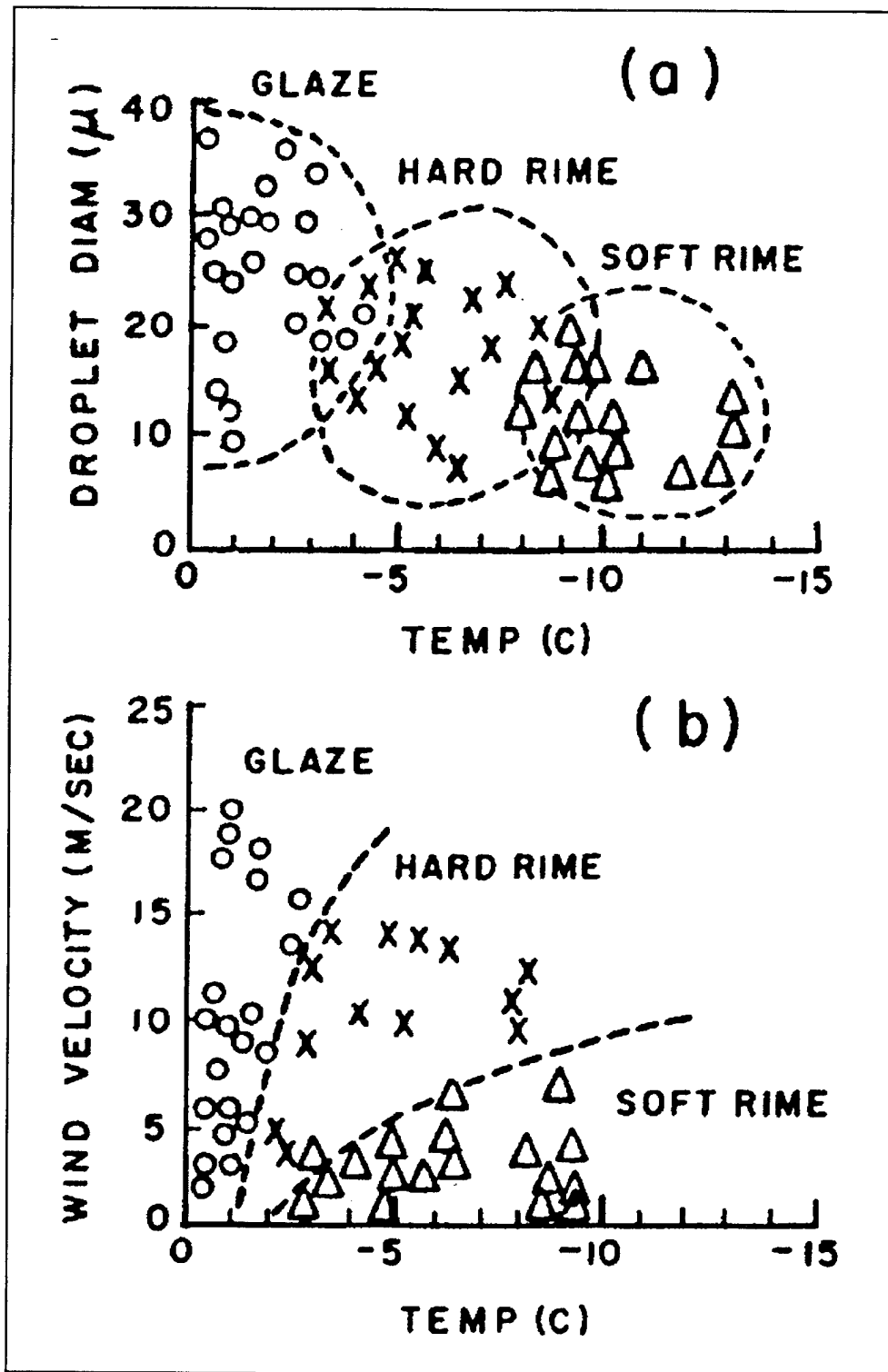


Figure 4. Relationships of ice types with (a) droplet diameter, and (b) air temperature and wind speed (From Kuroiwa, 1965).

2.3 Ice Shapes. Both glaze and rime ice tend to build up on the windward side of objects exposed to supercooled water droplets. In general, the accumulation increases with increasing wind speed, but at some point the less dense ice blows off. Examples of ice shapes on cylindrical surfaces are shown in Figures 5 through 7. As shown in Figure 5, soft rime has a feathery appearance with the feathers pointing into the wind. The temperature range for soft rime formation is such that an individual supercooled water droplet is able to freeze and release the latent heat before the next droplet impinges. As a

result, the soft rime has many air pockets. For hard rime (Figure 6), the time for freezing is about equal to the impingement rate so that fewer air bubbles are trapped. In the case of glaze (Figure 7), the narrow temperature range in which it forms does not allow rapid release of latent heat from freezing. The impingement rate of supercooled water droplets exceeds the time required for complete freezing. In some cases, with the air temperature at or near freezing, some unfrozen liquid water will run back as shown and freeze or be removed by the wind.

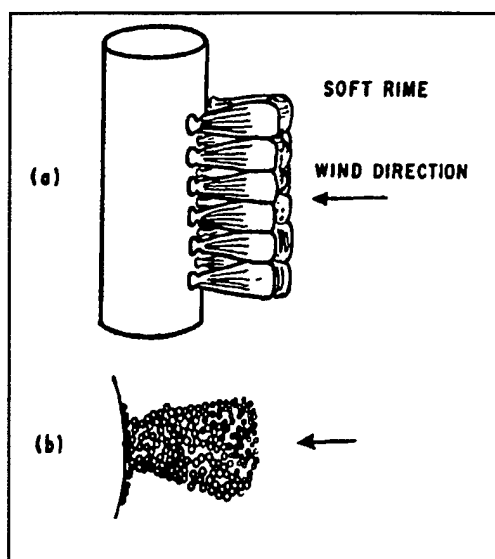


Figure 5. Shape of soft rime accretions on an object oriented normal to the wind flow; (a) side view and (b) from above (from Kuroiwa, 1965).

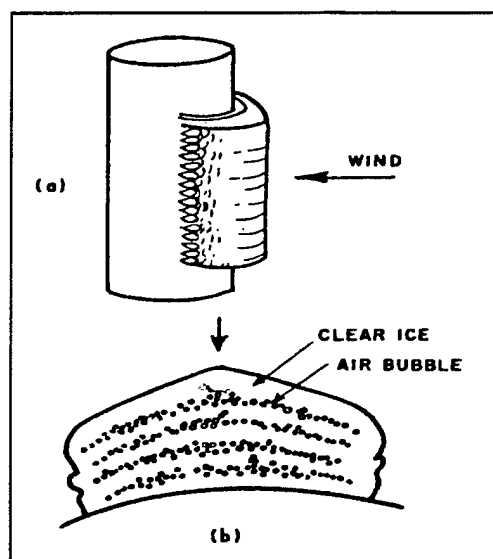


Figure 6. Same as Figure 5 except for hard rime.

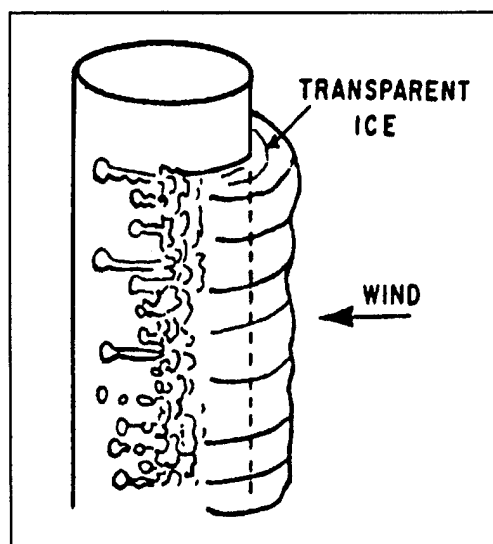


Figure 7. Same as Figure 5 except for glaze, side view only.

CHAPTER 2

2.4 Ice Accretion Theory. Because wires and cables are the usual items of concern regarding ice accretion near the surface, the theory of ice accretion is presented with respect to cylindrical objects. The next three paragraphs describe the basic theory on forces acting on droplets, collection efficiency, and equivalent radial thickness.

2.4.1 Forces on Droplets. As outlined by Chaine and Castonguay (1974), supercooled liquid water droplets carried in a wind flow as fog or clouds are acted on by two forces: *drag force* and *inertial force*. The drag force (F_d) makes the droplets follow the airflow. It is expressed as

$$F_d = \pi/2 (C_d \rho_a a^2 v^2) \quad (1)$$

where

ρ_a = air density

C_d = drag coefficient

v = relative velocity between the air and the droplets

a = radius of droplet

The inertial force (F_i) tends to keep the drops on a straight line, and is given by

$$F_i = Ka^3 \rho_w (dv/dt) \quad (2)$$

where K = storm specific constant

ρ_w = droplet density

dv/dt = rate of change of relative velocity

Equations 1 and 2 show that droplet size has a large effect on the inertial force. Larger droplets are deflected less than smaller ones. However, a large object will deflect more droplets due to the increased drag coefficient.

2.4.2 Collection Efficiency. As defined in Chaine and Castonguay (1974), the collection (catch) efficiency (E) is given by the ratio of the frontal projection of the water droplets to the diameter of the cylindrical object impinged upon.

$$E = y/D_o \quad (3)$$

where y = frontal projection of droplets on a trajectory that impinges on the cylinder

D_o = diameter of the cylinder

It can be seen from Equation 3 and Figure 8 that if the frontal projection is constant and the diameter of the collecting object decreases, the collection efficiency is increased. Given the same frontal projection, a larger object will deflect droplets at a greater distance in front of the cylinder, because the air flow is forced to flow around the cylinder due to drag. As a result, larger diameter objects capture less of the droplets and thus accumulate less ice.

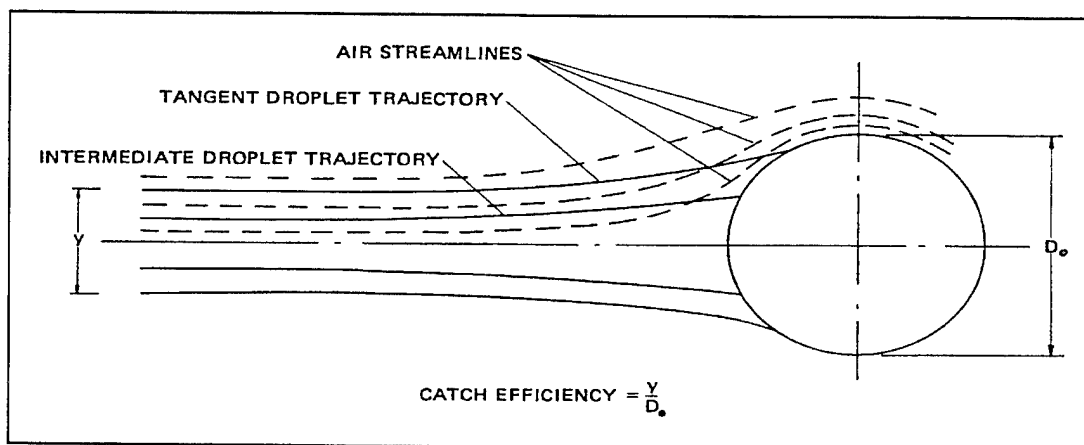


Figure 8. Collection (Catch) efficiency of a cylinder (from Chaine and Castonguay, 1974).

2.4.3 Equivalent Radial Thickness. The equivalent radial thickness (wherein it is assumed that ice accumulates uniformly around a cylinder) is a concept convenient for determination of ice loads. The ice thickness estimates for a 1/2-inch radius wire, given on USAFETAC Form 3, are equivalent radial thicknesses. In nature, ice accumulation on wires is not often uniform. Some examples are shown in Figure 9. In the idealized case (rotating), the wire is able to twist in the wind and ice is accreted uniformly. Ice accretions with cylindrical shapes actually do occur where winds are steady and the wire twists in reaction to changing ice mass. For a stationary wire with 100-percent collection efficiency, the ice accretion has a crescent shape on the windward side. In the typical case of a stationary wire with a collection

efficiency less than 100 percent, the ice accretion has a bell shape toward the wind.

As discussed by Tattelman (1979), many variations in ice accretion shape are possible due to changing temperature and wind speed, and variations in the geometry of surface structures. In this report (refer to Figure 9, rotating case), the equivalent radial ice thickness (T_R) is given by

$$T_R = R_1 - R_2 \quad (4)$$

where R_1 = radius of combined cylinder and ice

R_2 = radius of cylinder

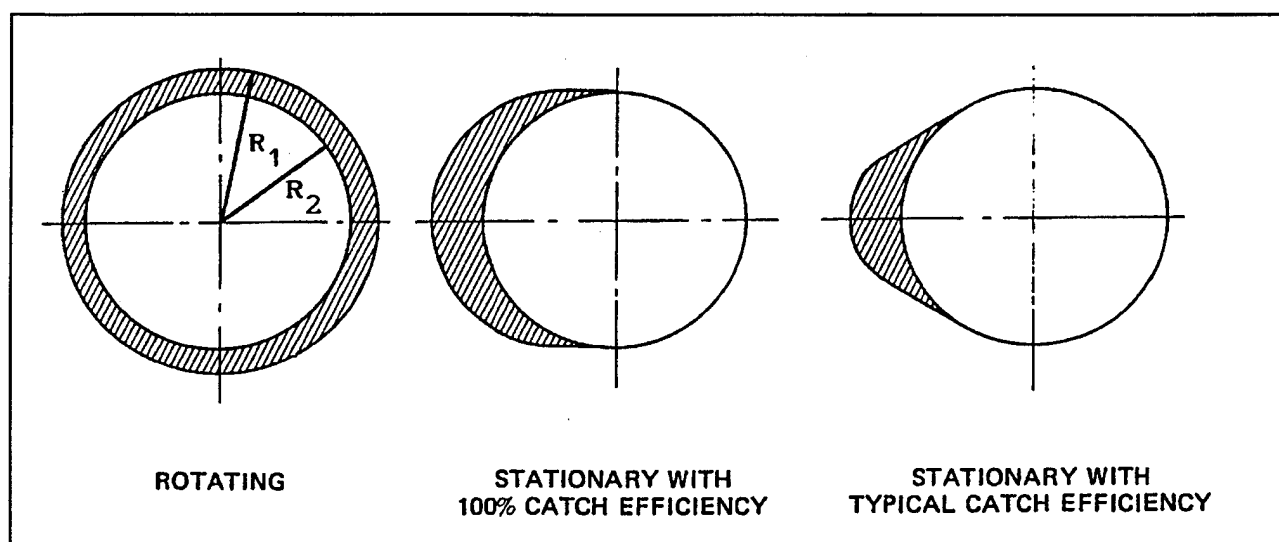


Figure 9. Variations in shapes of ice accumulations on wires (adapted from Chaîne and Castonguay).

2.5 Ice Accretion Models. As stated by several authors, modeling of ice accretion on surface objects is necessary because there are no routine and standardized observations of icing. As a result, empirical and theoretical models are used to estimate ice accretion from regularly observed atmospheric variables, and from specialized observations of drop size and liquid water content.

A brief description of over 20 ice accretion models is given by Henry (1987). According to Dr. Charles C. Ryerson at the U.S. Army Cold Regions Research and Engineering Laboratory (personal communication, 1993), none of the models have been adequately tested

by actual ice accretion observations. Some limited testing of models, however, has been done by Yip and Mitten (1991). Of the nine models they evaluated, one by Chaîne and Skeates (1974) was the best at predicting glaze ice accretion. A model by Makkonen (1984b) was second, but Makkonen's model was better than any of the others at predicting rime ice accretion. Only nine cases of rime icing were available for testing the models. The following paragraphs discuss the Chaîne and Skeates (1974) model; the Makkonen (1984b) model; and a model by McComber and Govoni (1985) that appears to be useful for predicting rime and glaze accretions.

CHAPTER 2

2.5.1 Chaine and Skeates Model. This model is in operational use at the Canadian Climate Centre (Yip, 1993). It is based on formulations by McKay and Thompson (1969). For horizontal surfaces (e.g., flat plates), the thickness (T_H) in inches is assumed equal to the observed liquid water equivalent amount measured for the total number of hours when either freezing or liquid precipitation occurred, and the temperature was at or below freezing. It is also assumed that all precipitation accretes as ice so that

$$T_H = Ph \quad (5)$$

where P = precipitation rate (in h^{-1})

h = precipitation duration in hours

As noted by McKay and Thompson (1969), the glaze ice accretion on surfaces at angles to the wind may exceed the precipitation rate. To estimate the vertical ice accretion thickness (T_V) in inches, it was assumed that the rate of increase in mass of a glaze layer, forming on a square meter flat surface normal to the wind, was related to the rainfall rate so that

$$T_V = 0.078v(P^{0.88})h \quad (6)$$

where v = average wind speed (mi h^{-1})

P = precipitation rate (in h^{-1})

h = precipitation duration in hours

It was also assumed that the collection efficiency of the vertical flat plate was 100 percent. That assumption may overestimate T_V , but it does allow for a worst case scenario. As a last step, the equivalent radial thickness (T_R) of glaze in inches for a wire is given by

$$T_R = [KR_2/2(T_H^2 + T_V^2)^{1/2} + R_2^2]^{1/2} - R_2 \quad (7)$$

where K = correction factor depending on the wire diameter

R_2 = radius of wire (inches)

T_H = horizontal glaze thickness (inches)

T_V = vertical glaze thickness (inches)

Note that the bracketed term in Equation 7 is equivalent to R_1 in Equation 4. The correction factor (K) is the ratio of experimentally determined ice deposits on cylinders of various sizes to theoretical calculations (Chaine and Castonguay, 1974).

A graph of K values for various wire diameters and temperature ranges is shown in Figure 10. A reference line for a 1-inch diameter wire is shown for convenience (refer to Figure 1).

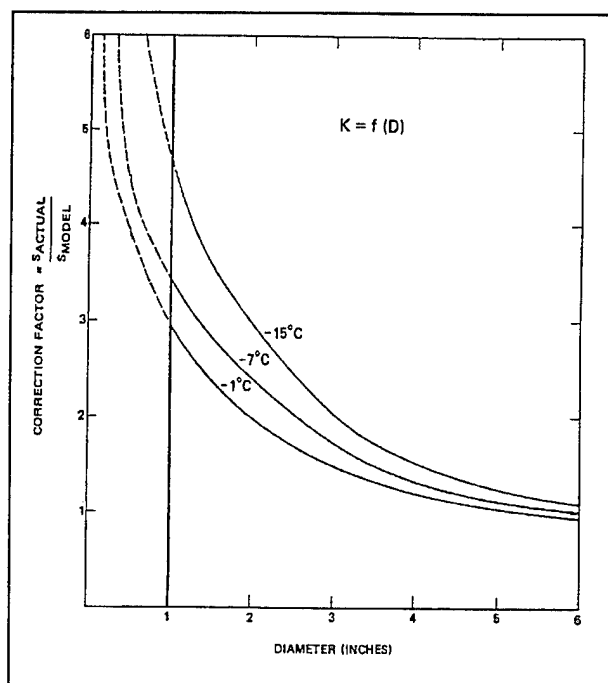


Figure 10. Correction factors (K) for various wire diameters and temperature ranges (adapted from Chaine and Castonguay, 1974).

2.5.2 Makkonen Model. Makkonen (1984b) developed a theoretical ice accretion model to reveal the basic physical processes that control icing on wires. The model is time-dependent and uses constant wind speed, air temperature, liquid water content, and median-volume droplet diameter as inputs. The droplets are assumed to move horizontally in the wind flow and impinge on a wire oriented normal to the flow. The model simulates glaze (wet growth) or rime (dry growth) ice accretion of supercooled water droplets onto the wire. In wet growth, there is some runoff from the ice deposit (refer to Figure 7). It is assumed that the runoff is shed into the wind at the edges of the wire. In dry growth, there is no runoff. All of the impinging supercooled water turns into ice on the wire. The icing intensity on the wire is given by

$$I = 2\pi(Envw) \quad (8)$$

where I = icing intensity ($\text{g cm}^{-2} \text{h}^{-1}$)

E = collection efficiency of the wire

n = freezing fraction; the fraction of supercooled water captured by the wire that turns to ice

($n < 1$ in wet growth; $n = 1$ in dry growth)

v = wind speed (m s^{-1})

w = liquid water content (g m^{-3})

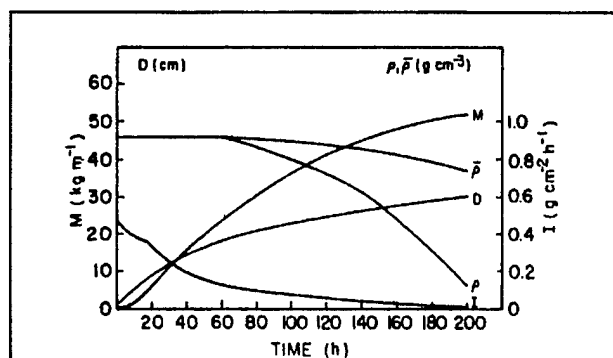


Figure 11. Results of numerical simulation of ice accretion on a 1-cm diameter wire. The simulated quantities are ice load (M), ice deposit diameter (D), density of accreting ice (ρ), total deposit density ($\bar{\rho}$), and the icing intensity (I). Input wind speed is 20 m s, air temperature is -1°C , liquid water content is 0.3 g m, and median-volume droplet diameter is 25 (ρ_{mv}) meters (adapted from Makkonen, 1984b).

At each 10-minute time step, the model simulates the quantities E , n , and I . It also simulates the diameter (D) of the ice deposit in cm; the ice load (M) in kg m^{-1} ; the density of the ice accretion in one time step, and the density of the total accretion, both in g cm^{-3} . Examples of a simulation are shown in Figures 11 and 12. In Figure 11, the ice deposit diameter (D) increases nonlinearly with time while the icing intensity (I) decreases nonlinearly with time. As the overall diameter (wire and ice) increases, the collection efficiency (E), and hence the icing intensity, decreases nonlinearly with time as seen in Figure 12. The ice load (M) increases nonlinearly with time (Figure 11), and emphasizes the importance of the duration of the icing.

The model also showed features of the ice accretion process on wires that had not been revealed by previous theories on ice accretion. For example, Figure 12 shows that the growth regime may change from wet ($n < 1$) to dry ($n = 1$) even under constant atmospheric conditions. Figure 11 shows that the ice density eventually decreases with time after dry growth is reached.

As Makkonen's (1984b) model shows, the process of ice accretion on wires is complex and not easily described with routinely measured atmospheric variables. The model can be used with varying input values, but adequate observations are not regularly available.

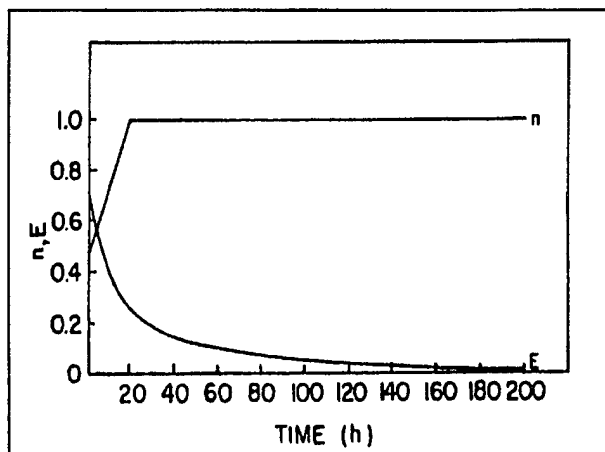


Figure 12. Time-evolution of the freezing fraction (n) and the collection efficiency (E). For a numerical simulation of ice accretion on a 1-cm diameter wire with input variables as in Figure 11 (adapted from Makkonen, 1984b).

CHAPTER 2

2.5.3 McComber and Govoni Model. McComber and Govoni (1985) conducted ice accretion experiments at Mount Washington, New Hampshire, in 1978 and 1980. The experiments were done with a 0.64-cm diameter stranded steel cable at 2.5 meters above ground, stretched between supports 6 meters apart, and oriented normal to the prevailing winds.

Measurements were taken of temperature, wind speed, liquid water content, droplet size, ice load, and maximum ice accretion diameter. Of five icing events selected for analysis, an increasing icing rate with time was observed in all cases. That finding contrasted with the Makkonen (1984b) model results that showed a decreasing icing rate (i.e., icing intensity) with time. Furthermore, none of the other models discussed by Makkonen (1984b) readily fit the data from the five icing events. Therefore, McComber and Govoni (1985) suggested an exponential growth model

$$M = M_0 e^{kt} \quad (9)$$

where M = ice load per unit length (kg m^{-1})

M_0 = initial ice load (kg m^{-1})

k = constant

t = duration of icing (h)

In Equation 9, the constant (k) is given by

$$k = [3.54 \times 10^{-2} (EwV_m)] / \rho_i D_0 \quad (10)$$

where E = collection efficiency

w = liquid water content (g m^{-3})

V_m = average wind speed (m s^{-1})

ρ_i = ice accretion density (g m^{-3})

D_0 = diameter of wire (m)

The ice load (M) in Equation 9 is related to the ice accretion diameter (D) by

$$M = (0.785 D^2) / \rho_i \quad (11)$$

from which the ice accretion diameter (D), in meters, is given by

$$D = (\rho_i M / 0.785)^{1/2} \quad (12)$$

McComber and Govoni (1985) found that their measured data fits well to the exponential growth model. The average initial ice load (M_0) for the five icing events was 1.0 kg m^{-1} .

Chapter 3

METHODS FOR ESTIMATING ICING

3.1 General Considerations. An excellent starting point in making an estimate of ice accretion on surface structures is a review of historical files on engineering design information prepared by USAFETAC's Engineering Meteorology Section. The files contain icing estimates for specific locations (on USAFETAC Forms 3; see Figure 1) and background information by country. As part of the search for climatological data for the area of interest, a literature review specific to the area on icing would be helpful. The search should include an evaluation of synoptic weather patterns that affect the area. Locations along the major winter storm tracks are especially prone to icing, as are locations exposed to long fetches of moisture-laden air. Other considerations are topography of the area and exposure of the location to the prevailing wind flow. As a rule, locations on the windward side of hills and mountains exposed to cloud systems that contain supercooled water droplets are most vulnerable to icing.

In the following recommendations on estimating icing, it is assumed that the phenomenon of icing on surface structures is the same worldwide, and that the estimation methods apply anywhere.

3.2 Glaze Estimates from Freezing Precipitation. The estimates described in this section are intended for use where the elevations of the observing location and location of interest differ by less than 1,000 meters. This is because Equation 13 is valid only in the planetary boundary layer. Locations above the planetary boundary layer are more likely to experience glaze ice from in-cloud processes as discussed in the next section. If surface weather observations are available at the location of interest, or from nearby locations that are considered representative, the model by Chaine and Skeates (1974) is recommended for glaze thickness estimates. In the typical case where the location of interest is away from the observing locations, proceed as follows to obtain flat plate glaze thickness estimates:

- Assume that the precipitation rate and duration at the location of interest are the same as at the observing location.

- Obtain the liquid equivalent precipitation amounts for each period in where the temperature was at or below freezing.

- Obtain the average temperature and wind speed for each period.

- Use Equation 5 to estimate the glaze thickness on a flat plate for each period.

- Use the highest annual thickness value for each year from as many years of record as possible, and do an extreme value analysis (refer to Air Weather Service, 1977) to obtain the flat plate glaze thickness for a 95-year return period.

For glaze thickness on a 1/2-inch radius wire, if the location is at an elevation higher than the observing station, it will be necessary to estimate the average temperature and mean wind speed at the location of interest.

- Use the moist adiabatic lapse rate ($0.5^{\circ}\text{C}/100\text{ m}$) to adjust the average temperature.

- Use the following equation from Thom (1970) to adjust the average wind speed:

$$v_2 = v_1 [(z_2/z_1)]^{1/7} \quad (13)$$

where v_2 = wind speed at location of interest (mi h^{-1})

v_1 = wind speed at observing location (mi h^{-1})

z_2 = elevation of location of interest (feet)

z_1 = elevation of observing location (feet)

CHAPTER 3

- Use Equation 6 to estimate the vertical glaze thickness.
- Use Equation 7 and Figure 10 to estimate the equivalent radial thickness of glaze on the wire.
- Use the highest annual equivalent radial thickness values as input for an extreme value analysis to obtain the 95-year return period thickness.

If the location of interest is too far from observing stations, it will be necessary to estimate glaze amounts from previous estimates. In any case, the glaze ice thickness values for the United States in Table 2, and the Ice Accretion Handbook by Chaîne and Skeates (1974) for glaze ice in Canada, are good references.

3.3 In-Cloud Rime and Glaze Estimates. If the location of interest is in hilly or mountainous terrain, and frequently enshrouded with clouds, it is more likely to experience rime icing than glaze icing. However, either type (or mixtures of both) are possible on a surface object, depending on the air temperature and size of supercooled water droplets in the cloud that impinge on the object. The wind speed and liquid water content are also important factors that affect ice type.

The exponential growth model by McComber and Govoni (1985) is recommended to estimate in-cloud rime and glaze on a 1/2-inch radius wire. For the flat plate estimate, the following general relationship between vertical and horizontal ice accumulations from Chaîne and Castonguay (1974) is recommended:

$$T_H = 10T_V/V \quad (14)$$

where T_H = horizontal ice thickness (inches)

T_V = vertical ice thickness (inches)

V = mean wind speed (miles h⁻¹)

Input for the McComber and Govoni (1985) model requires estimation of several variables.

3.3.1 Estimation of Input variables. As a first step, use a representative upstream observing station to determine the following for each year of record:

- For each month of the year, determine the maximum number of consecutive hours that the ceiling was below the level of the location of interest. Depending on the latitude and elevation of the location of interest, it may experience in-cloud icing in every month.
- If the maximum number of hours occurs more than once in any month, keep all periods.
- Calculate the average air temperature and average wind speed for each period.
- Obtain an estimate of the average air temperature at the location of interest by reducing the average air temperature at the observing station according to the moist adiabatic lapse rate (0.5° C/100 meters). It can be seen in the study by Schaub (1981) that the temperature lapse rate (from the surface to the site on Monte Cimone) more closely followed the moist adiabatic rate during the severe in-cloud icing event.
- Obtain an estimate of the average wind speed at the location of interest by using Equation 13 as a guide for locations up to 1,000 meters above the observing location. For higher locations, assume a linear increase in average wind speed based on the calculated rate of increase from the observing location to 1,000 meters above the observing location.
- Eliminate periods in which the average air temperature at the location of interest is above 0°C or below -10°C (refer to Table 3 and Figure 4). Soft rime that forms at temperatures below -10°C is usually removed by the wind before much accumulates.
- Separate the remaining periods according to average temperature at the location of interest. If the average temperature is from 0°C to -3°C, the period is one of *glaze* ice accretion; otherwise, the period is one of *rime* ice accretion.
- Keep the longest glaze period and rime period. The length of each period in hours is the duration (t) for use in Equation 9.

To obtain an estimate for the constant (k) in Equation 9, it is necessary to assume constant average values for collection efficiency (E), liquid water content (w), ice accretion density (ρ_i) and wind speed (V_m). Based on simulations by Makkonen (1984b) and calculations McComber and Govoni (1985), an average collection efficiency of 0.1 is assumed for a wire with a diameter (D_o) of 2.54×10^{-2} m (1 inch).

To estimate average liquid water content, it is generally agreed (Makkonen, 1984a) that glaze is favored when liquid water content is high. Patnoe and Tank (1993) described aircraft measurements of liquid water content during the winter of 1992 in the North Atlantic near the maritime provinces of Canada. A maximum supercooled liquid water content of 1.2 g m^{-3} was measured in clouds from 7,000 to 8,000 feet MSL. From aircraft measurements in Colorado, Bernstein and Politovich (1993) reported that mixed (glaze and rime) icing occurred where the supercooled liquid water content exceeded 0.6 g m^{-3} in clouds around 9,000 feet MSL.

McComber and Govoni (1985) measured a liquid water content of 1.4 g m^{-3} during a freezing rain event on Mount Washington at an elevation of 6,265 feet MSL. In this report, an average liquid water content of 0.8 g m^{-3} is assumed for glaze ice accretion. For rime ice accretion, an average of 0.4 g m^{-3} is assumed as a compromise between measurements by McComber and Govoni (1985) of 0.5 g m^{-3} , and the maximum liquid water content of 0.3 g m^{-3} in mountain fog (Makkonen, 1984a). For ice accretion density, average values of 0.8 g cm^{-3} for glaze and 0.3

g cm^{-3} for rime were obtained from Table 3. Estimates of average wind speed can be made as described in 3.3.1.

3.3.2 Application of McComber and Govoni Model.

Use Equation 10 to obtain a value for the constant (k) for the longest duration (t) of in-cloud glaze and rime ice accretion for each year of record. Calculate the ice load (M) from Equation 9, assuming that the initial ice load (M_o) is 1.0 kg m^{-1} . Use Equation 12 to obtain the glaze and rime ice accretion diameters (D) for each year of record. Convert the values of D to cm and use the equation below to obtain the equivalent radial glaze and rime ice thicknesses on a 1/2-inch radius wire.

$$T_R = (D - 2.54)/2 \quad (15)$$

where T_R = equivalent radial ice thickness (inches)

D = ice accretion diameter (cm)

To estimate glaze and rime ice thicknesses on a flat plate (T_H) for each year of record, use the following equation:

$$T_H = 10T_R/V_m \quad (16)$$

where T_R = equivalent radial ice thickness from equation 15 (inches)

V_m = average wind speed at location of interest (mi h^{-1})

3.4 What to Expect. It appears that in-cloud icing occurs with more regularity than glaze ice events from freezing precipitation. As an example, consider the icing data in Table 4 and the extreme value analysis of icing in Figure 13, next page, for Monte Cimone, Italy, at an elevation of 7,101 feet MSL. The input data consisted of maximum annual ice thicknesses for 1971-78 obtained by USAFETAC's Engineering Meteorology Section in 1979 from Italian military sources. The type of ice was not given, but mostly rime can be assumed. It can also be assumed that the accretions were on objects oriented at various angles to the wind flow. It is important to note that due to the consistency in annual maximum ice amounts (Table 4), the 95-year return period value of nearly 200 cm (Figure 13) is not particularly large in comparison.

Other locations in hilly and mountainous areas experience similarly large ice accumulations. As noted by Putnam (1991), the great ice storm of January 8-13, 1956," on Mount Washington (elevation 6,265 feet MSL) in New Hampshire left ice thicknesses of 12-

18 inches near the ground on windward sides of buildings, and thicknesses of 6 feet on the top of a 100-foot tower. The tower, which still stands, was designed to withstand a wind of 300 miles h^{-1} with a 6-foot ice accumulation.

On the Brocken (elevation 3,747 feet MSL), the highest point of the Harz Mountains in Germany, rime ice has been seen to accumulate at the rate of 50 cm in 24 hours, and at one time a telegraph pole was covered by a rime thickness of nearly 3 meters.

Although not as regular from year to year as in-cloud icing, extreme accumulations of glaze ice at lower elevations from freezing precipitation are also impressive, as noted in Table 2. Page (1969) gave an example of a heavy glaze ice event in the United Kingdom that caused the collapse of a 1,250-foot tower due to a 4-inch radial accumulation on the guy wires. Other notable examples occurred in eastern Newfoundland (Boyd, 1970) and Nova Scotia (McKay and Thompson, 1969), generally considered the worst locations on earth for glaze ice accumulations.

Table 4. Annual maximum ice thickness (cm) for Monte Cimone, Italy, elevation 7,101 feet.

	Year							
	1971	1972	1973	1974	1975	1976	1977	1978
Thickness	130	136	130	136	150	120	150	130
Month	Feb	Mar	Mar	Feb	Feb	Feb/Dec	Jan	Feb

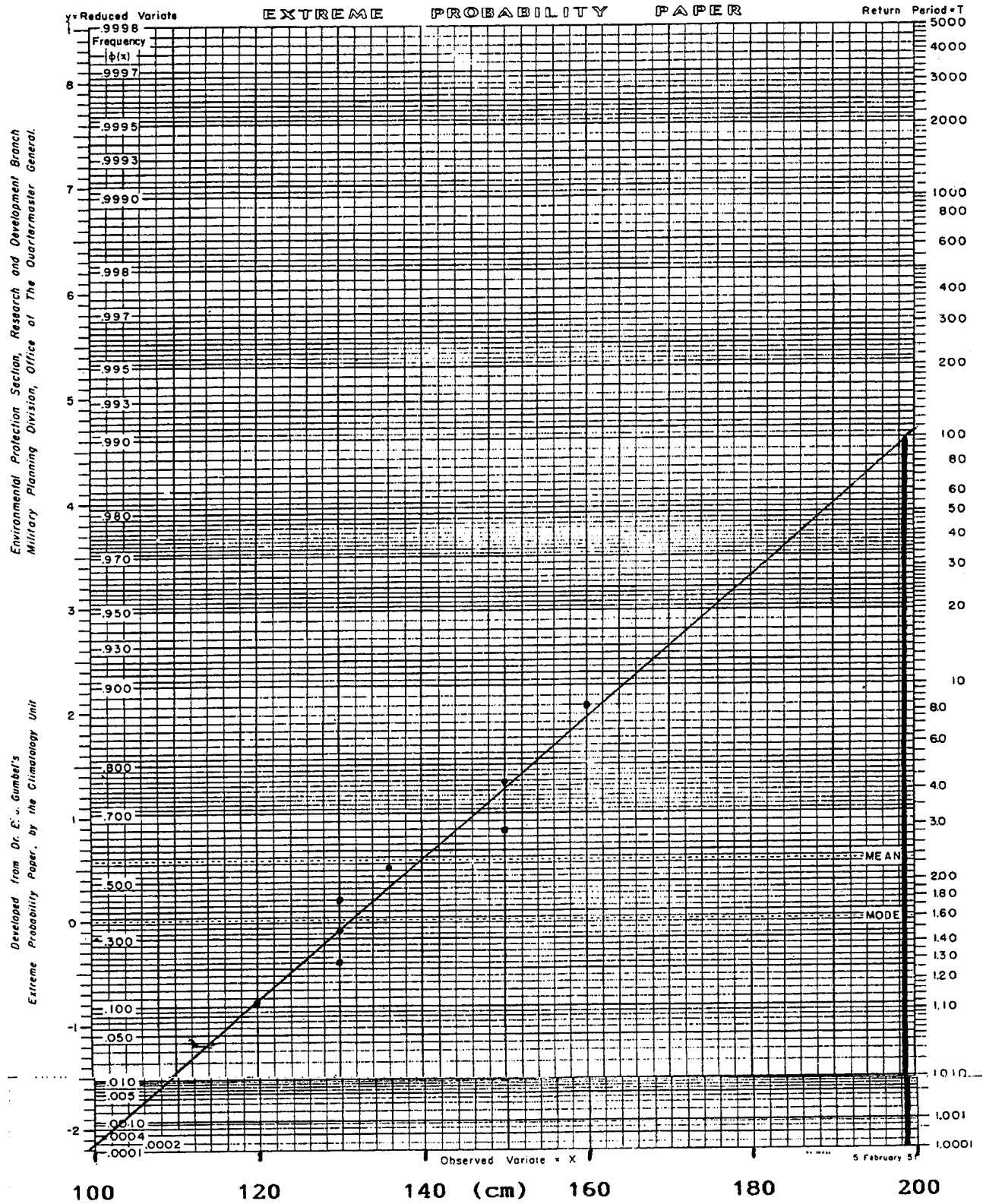


Figure 13. Extreme value analysis of annual maximum ice thickness (cm) for Monte Cimone, Italy. Input data from Table 4. The 95-year return period value is read where the bold vertical line intersects the abscissa.

Do an extreme value analysis on the annual maximum glaze and rime thicknesses for a 1/2-inch radius wire and a flat plate (Air Weather Service, 1977) to obtain the 95-year return period values for entry on USAFETAC Form 3 (Figure 1).

3.5 Variations of Ice Thickness on Tall Structures. The example of tower icing on Mount Washington shows that ice accumulations tend to increase with height above the surface. Caspar and Sandreczki (1964) deduced from 13 years of data on ice accretion in Europe that the amount of ice was generally two to three times greater at a height of 16 meters above the ground than at 2 meters. Ryerson (1987) found, from observations on Mount Mansfield, Vermont (elevation 4,021 feet), during two winters, that in some cases rime ice thicknesses on towers *doubled* from 2 meters above ground up to 30 meters. Generalities like these can be misleading, because the shape and orientation of the iced surfaces is not specified. Glukhov (1972) used data from a 300-meter meteorological tower at Obninsk near Moscow to show how the average diameters of glaze and hard rime on wires increase with increasing height. The average diameters of both ice types roughly double at 200 meters above ground, and increase by five to six times the surface values at 300 meters above ground (Figure 14). Minsk (1977) surmised that the findings of Glukhov (1972) hold true for any location. On USAFETAC Form 3, it is recommended that Figure 14 be used as a guide in adjusting ice thickness estimates for tall structures.

3.6 Maximum Wind with Ice Loads. Winds that can damage a structure loaded with ice usually occur after the ice is deposited. In a typical example, ice is deposited on a structure in advance of a cold front, and subsequent strong winds behind the front further stress the ice loaded structure. Therefore, an extreme value analysis of wind speeds coincident with ice accretion may not produce representative results. For that reason, Tattelman and Gringorten (1973) used

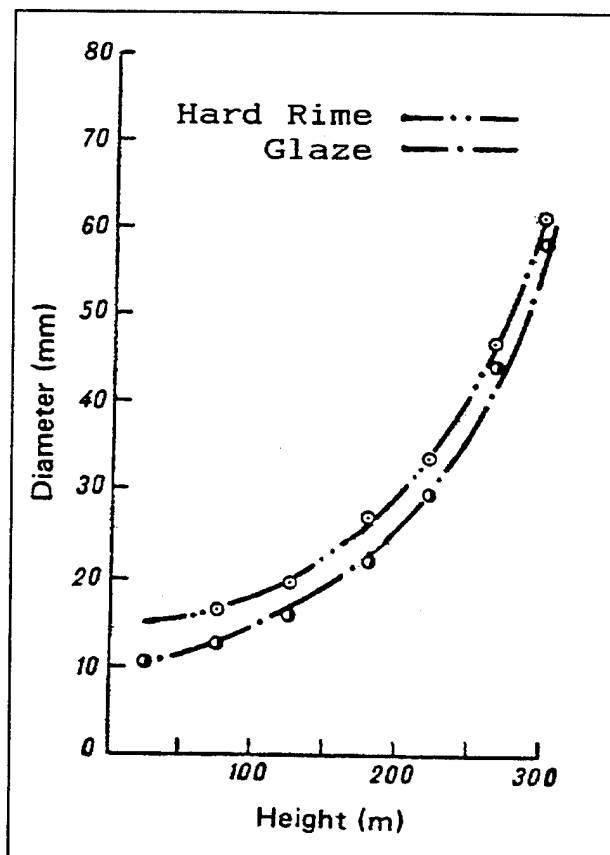


Figure 14. Variation of average diameters of glaze and hard rime accumulations with height above ground (adapted from Glukhov, 1972).

peak gusts from days below freezing after an icing event to determine maximum winds with ice load. Chaine and Skeates (1974) used the wind speed observed during an ice storm, and for that part of the 24-hour period after the storm that the temperature was below freezing. McKay and Thompson (1969) found that extreme value analyses of wind speeds during and 24 hours after icing events produced lower values than extreme value analyses based on all wind speeds. To estimate the maximum wind with ice loads, it is recommended that annual peak gusts for only the month(s) that the annual maximum ice accumulations occurred be used as input to an extreme value analysis to obtain the 95-year return period value.

Chapter 4

CONCLUSIONS

The methods proposed in this report to estimate ice accumulations demonstrate the difficulties encountered when forced to make estimates of infrequently measured phenomena from regularly observed meteorological variables.

Faced with a lack of observations in hilly and mountainous locations, where structures such as communications towers are commonly sited, it is necessary for one to make tough determinations of

icing duration, ice type, liquid water content, and so forth.

The method for estimating glaze amounts from freezing precipitation can be automated with relatively simple software development, but the method for estimating in-cloud rime and glaze amounts requires more detailed programming. Feedback on icing events at manned locations is needed to verify and improve ice accumulation estimates.

REFERENCES

- Air Weather Service : *Guide for Applied Climatology*. AWS-TR-77-267, AD-A052 579, Air Weather Service, Scott AFB, IL, 1977.
- Bennett, I. : *Glaze - Its Meteorology and Climatology, Geographical Distribution, and Economic Effects*. Environmental Research Division, Technical Report EP-105, HQ Quartermaster Research and Engineering Center, Natick, MA, 1959.
- Bernstein, B.C. and M.K. Politovich: "The Production of Supercooled Liquid Water by a Secondary Cold Front." *Preprints, Fifth International Conference on Aviation Weather Systems*, American Meteorological Society, Boston, MA, pp. 422-426, 1993.
- Boyd, D.W. : *Icing of Wires in Canada*. National Research Council of Canada, Technical Report No. 317, Ottawa, Canada, 1970.
- Caspar, W. and A. Sandreczki : *Ice Deposits from the Meteorological Standpoint Sonderdruck aus Elektrotechnische Zeitschrift*, Ausgabe B, Bd. 16, S. pp. 763-767, 1964.
- Chaine, M., and G. Castonguay: "New Approach to Radial Ice Thickness Concept Applied to Bundle-like Conductors." *Industrial Meteorology - Study IV*, Environmental Canada, Toronto, Canada, 1974.
- Chaine, P.M., and P. Skeates: "Ice Accretion Handbook (freezing precipitation)." *Industrial Meteorology Study VI*, Environmental Canada, Toronto, Canada, 1974.
- Glukhov, V.G.: "Meteorological Conditions for Formation of Ice on High Structures (in Russian)." Leningrad: *Gidrometeoizdat, Trudy*, Vol 311, G.G.O., 1972.
- Henry, K.: "Atmospheric Icing of Transmission Lines." *Cold Regions Technical Digest No. 87-2*, Cold Regions Research and Engineering Laboratory, Hanover, NH, 1987.
- Kuroiwa, D.: *Icing and Snow Accretion on Electric Wires*. CRREL Res. Rep. No. 123, Cold Regions Research and Engineering Laboratory, Hanover, NH, 1965.
- Makkonen, L.: *Atmospheric Icing on Sea Structures*. CRREL Monograph No. 84-2, Cold Regions Research and Engineering Laboratory, Hanover, NH, 1984a.
- Makkonen, L.: "Modeling of Ice Accretion on Wires." *J. Clim. Appl. Meteor.*, 23, pp. 929-939, 1984b.
- McComber, P., and J.W. Govoni: "An Analysis of Selected Ice Accretion Measurements on a Wire at Mount Washington." *Proceedings of the Forty-Second Annual Eastern Snow Conference*, Montreal, Canada, 1985.
- McKay, G.A., and H.A. Thompson: "Estimating the Hazard of Ice Accretion in Canada from Climatological data." *J. Appl. Meteor.* 8, pp. 927-935, 1969.
- Minsk, D.L.: *Ice Accumulation on Ocean Structures*. CRREL Rep. No. 77-17 Cold Regions Research and Engineering Laboratory, Hanover, NH, 1977.
- Page, J.K.: "Heavy Glaze in Yorkshire - March 1969." *Weather*, 24, No. 12, pp. 486-495, 1969.

- Patnoe, M.W., and W.G. Tank: "Airplane Icing Research at the Boeing Company: Participation in the Second Canadian Atlantic Storms Program." *Preprints, Fifth International Conference on Aviation Weather Systems*, American Meteorological Society, Boston, MA, pp. 432-434, 1993.
- Putnam, W.L.: *The Worst Weather on Earth*. Mount Washington Observatory, Inc., Gorham, NH, and The American Alpine Club, New York, NY, 1991 .
- Rasmussen, R.M., and I. Baker: "Preliminary Studies of Ice Formation in Upslope Clouds." *Preprints, Fifth International Conference on Aviation Weather Systems*, American Meteorological Society, Boston, MA, pp. 440-443, 1993.
- Ryerson, C.C.: *Rime Meteorology in the Green Mountains*. CRREL Rep. No. 87-1, Cold Regions Research and Engineering Laboratory, Hanover, NH, 1987.
- Schaub, W.R., Jr.: "Case Study of Severe Icing on Monte Cimone in the Apennine Mountains of Italy." *Preprints, Second Conference on Mountain Meteorology*, American Meteorological Society, Boston, MA, pp. 41-45, 1981.
- Tattelman, P.: *Climatic Chamber Tests of a Surface Ice Accretion Measurement System*. AFGL-TR-79-0079, Hanscom AFB, MA, 1979.
- Tattelman, P., and I.I. Gringorten: *Estimated Glaze Ice and Wind Loads at the Earth's Surface for the Contiguous United States*. AFCRL-TR-73-0646, Hanscom AFB, MA, 1973.
- Thom, H.C.S.: "Engineering Climatology of Design Wind Speeds with Special Application to the Chicago Area." *Proceedings of the Chicago Design Symposium*. Northwestern University, Evanston, IL, pp. 17-34, 1970.
- Yip, T.C.: "Estimating Icing Amounts Caused by Freezing Precipitation in Canada." *Proceedings of Sixth International Workshop on Atmospheric Icing of Structures*, Budapest, Hungary.
- Yip, T.C., and P. Mitten,: "Comparisons Between Different Ice Accretion Models." *Canadian Electrical Association, Engineering and Operating Transactions*, 30, Toronto, Canada, 1991.

GLOSSARY

a	droplet radius	ρ_w	droplet density
C	Celsius	R_1	radius of combined cylinder and ice
C_d	drag coefficient	R_2	radius of cylinder
cm	centimeters	s	second
D	ice deposit diameter	t	time, duration of icing
D_o	diameter of cylinder or wire	T_H	horizontal ice thickness
E	collection efficiency	T_R	equivalent radial ice thickness
F_d	drag force	T_V	vertical ice thickness
F_i	inertial force	μm	micron (10^{-6} m)
g	grams	USAFETAC	USAF Environmental Technical Applications Center
I	icing intensity	v	wind speed, relative velocity between the air and the droplets
k	constant	v_1	wind speed at observing station
K	storm specific constant, correction factor depending on wire diameter	v_2	wind speed at location above observing station
kg	kilograms	V, V_m	mean or average wind speed
M	ice load	w	liquid water content
M_o	initial ice load	y	frontal projection of droplets
n	freezing fraction	z_1	elevation of observing location
P	precipitation rate	z_2	elevation of location above observing location
ρ_a	air density		
ρ_i, ρ	total ice deposit density		

DISTRIBUTION

USAF XOWP 1490 AIR FORCE PENTAGON WASHINGTON DC 20330-1490	2
USAF/XOOOW 1490 PENTAGON RM BD927 WASHINGTON DC 20330-1490	1
OSAF SS 6560 PENTAGON RM 4C1052 WASHINGTON DC 20330-6560	1
AWS XO 102 WEST LOSEY ST SCOTT AFB IL 62225-5206	4
COMBAT WEATHER FACILITY, BLDG 91027 595 INDEPENDENCE RD BLDG 91027 HURLBURT FLD FL 32544-5618	1
OL K AWS NEXRAD OSF 3200 MARSHALL DR STE 100 NORMAN OK 73072-8028	1
OL N AWS C/O ARL (AMSRL-BE-W) BLDG 1646 RM 24 WHITE SANDS MSSL RNGE NM 88002-5501	1
AFGWC DO 106 PEACEKEEPER DR STE 2 N3 MBB 39 OFFUTT AFB NE 68113-4039	2
AWSTL FL4415 859 BUCHANAN ST SCOTT AFB IL 62225-5118	50
USAFETAC 859 BUCHANAN STREET SCOTT AFB IL 62225-5116	6
OL A USAFETAC FEDERAL BLDG RM 305 PAGE AVE ASHEVILLE NC 28801-2723	1
1ACC DOW 30 ELM STREET, STE 215 LANGLEY AFB VA 23665-20938	1
ACC DOWOE (WSU) 205 DODD AVE, STE 101 LANGLEY AFB VA 23665-2789	1
ACC AOS/AOW (WSU) 205 DODD AVE, STE 203A LANGLEY AFB VA 23665-84953	1
AFFOR/WX APO AA 34042-5000	1
JSOC WEATHER 32744 ALDISH DR FT BRAGG NC 28307-0239	1
THIRD US ARMY WEA TM BLDG 130 ANDERSON WAY FT MCPHERSON GA 30330-5000	1
USCENTAF/A3-DOOW 524 SHAW DRIVE SUITE 225 SHAW AFB SC 29152-5029	1
USSOUTHAF/A3-DOOSM 5325 EAST KACHINA ST DAVIS MONTHAN AFB AZ 85707-4921	1
WEATHER READINESS TRAINING CENTER (WRTC) PO BOX 465 RTE 1, CAMP BLANDING STARKE FL 32091-9703	1
NGB XOOSW MAIL STOP 18 ANDREWS AFB MD 20331-6008	1
AETC/XOSW 1F ST STE 2 RANDOLPH AFB TX 78150-4325	1
AFIT LDEE 2950 P ST BLDG 640 WRIGHT-PATTERSON AFB OH 45433-7765	1
AFIT CIR WRIGHT-PATTERSON AFB OH 45433-6583	1
AU/ACSC (MAJOR MUOLO/DEA) 225 CHENNAULT CIRCLE MAXWELL AFB AL 36112-6426	1
NAIC DXLA 4115 HEBBLE CREEK RD STE 9 WRIGHT-PATTERSON AFB OH 45433-5613	3
NAIC TATW 4115 HEBBLE CREEK ROAD STE 33 WRIGHT-PATTERSON AFB OH 45433-5637	1
AFCEA WE STOP 21 TYNDALL AFB FL 32403-6001	1
AFMC DOW 4225 LOGISTICS AVE STE 2 WRIGHT-PATTERSON AFB OH 45433-5714	1
AFOTEC/WE 8500 GIBSON BLVD SE KIRTLAND AFB NM 87117-5558	1
AL/OEBE ARMSTRONG LABORATORY 2402 EAST DRIVE BROOKS AFB TX 78235-5114	1
ASC/WE BLDG 91 3RD ST WRIGHT-PATTERSON AFB OH 45433-6503	1
ESC ENS 5 EGLIN ST HANSCOM AFB MA 01731-2116	1
ESC WE 5 EGLIN ST HANSCOM AFB MA 01731-2172	1
PL/TSML 5 WRIGHT ST HANSCOM AFB MA 01731-3004	1
PL/LI 3550 ABERDEEN AVE SE KIRTLAND AFB NM 87117-5776	2
PL WE 3550 ABERDEEN AVENUE KIRTLAND AFB NM 87117-5776	1
RL/WE 525 BROOKS RD GRIFFISS AFB NY 13441-4505	1
SMC SDEW 160 SKYNET ST STE 2315 LOS ANGELES CA 90245-4683	1
WL/DOWM 2130 8TH ST STE 11 WRIGHT-PATTERSON AFB OH 45433-7552	1
46 TW/TSWG 211 W EGLIN BLVD STE 128 EGLIN AFB FL 32542-5429	1
46 TEST GROUP WE 871 DEZONIA DRIVE BLDG 1183 HOLLOMAN AFB NM 88330-7715	1
USSPACECOM J3W 250 S PETERSON BLVD STE 116 PETERSON AFB CO 80914-3220	1
AFSPACECOM/DOGW 150 VANDENBERG ST STE 1105 PETERSON AFB CO 80914-4200	1
ADF WE STOP 77 18201 E DEVILS THUMB AVE AURORA CO 80011-9536	1
AFSFC SYT 715 KEPLER AVE STE 60 FALCON AFB CO 80918-7160	1
CAPE CANAVERAL FORECAST FACILITY/ROCC BLDG 81900 CAPE CANAVERAL AFS FL 32925-6537	1
DET 2 SMC/TDOR (WEATHER) 1080 LOCKHEED WAY BOX 044 ONIZUKA AFB CA 94088-1235	1
AMC/DOWR 402 SCOTT DR UNIT 3A1 SCOTT AFB IL 62225-5302	1
AMC/XOWX 402 SCOTT DR UNIT 3A1 SCOTT AFB IL 62225-5302	1
AMWC/WCOXI 5656 TEXAS AVENUE FT DIX NJ 08640-5000	1
TACC/WXF 402 SCOTT DRIVE RM 132 SCOTT AFB IL 62225-5029	1
15 AF DOW MARCH AFB CA 92518-5000	1
US ATLANTIC COMMAND 1562 MITSCHER AVENUE STE 200 NORFOLK VA 23551-2488	1
USAFALCENT RA POPE AFB NC 28308-5000	1
USCENTCOM CCJ3-W BLDG 540 MACDILL AFB FL 33608-7001	1
USCINCPAC (J37) BOX 13 CAMP H.M. SMITH HI 96861-5025	1

USEUCOM J3 OD WE UNIT 30400 BOX 1000 APO AE 09128-4209	1
USSOCCENT SCJ2- SWO 7115 S BOUNDARY DRIVE MACDILL AFB FL 33621-5101	1
USSOCOM SOJ3 OW 7701 TAMPA POINT BLVD MACDILL AFB FL 33621-5323	1
USSOUTHCOM SWO UNIT 0640 APO AA 34001-5000	1
USSTRATCOM J 315 901 SAC BLVD STE 1B29 OFFUTT AFB NE 68113-6300	1
USSTRATCOM/J3615 901 SAC BLVD STE 1F14 OFFUTT AFB NE 68113-6700	1
USTRANSCOM J3/4 OW 508 SCOTT DR BLDG 1900 SCOTT AFB IL 62225-5357	1
USTRANSCOM J5-SC (MITRE AFDIS) 508 SCOTT DR BLDG 1900 SCOTT AFB IL 62225-5357	1
6 SOPS/DOD 106 PEACEKEEPER DR STE 2N3 OFFUTT AFB NE 68113-4027	1
OL A SOCOS/WX BLDG AT 3275 BAY 50 FT BRAGG NC 28307-5203	1
NCDC LIBRARY FEDERAL BUILDING ASHEVILLE NC 28801-2733	1
NGDC/NOAA (ATTN: AF LIAISON OFFICER) MAIL CODE E/GC2 325 BROADWAY BOULDER CO 80333-3328	1
NIST PUBS PRODUCTION RM A635 ADMIN BLDG GAITHERSBURG MD 20899	1
NOAA/MASC LIBRARY MC5 325 BROADWAY BOULDER CO 80303-3328	1
NOAA CENTRAL LIBRARY 1315 EAST-WEST HIGHWAY SSMC E 2D FLOOR SILVER SPRING MD 20910	1
NWS W/OSD SSMC- 2 RM 12220 1325 EAST-WEST HIGHWAY SILVER SPRING MD 20910-3283	1
NWS W/OM21 1325 EAST-WEST HWY RM 13208 SILVER SPRING MD 20910	1
NWS W/OSD BLDG SSM C-2 EAST-WEST HWY SILVER SPRING MD 20910	1
PACAF DOW 25 E ST STE I232 HICKAM AFB HI 96853-5426	1
3 ASOS/GEW BLDG 1558 FT WAINWRIGHT AIN AK 99703-5200	1
3 OSS WE 7TH ST BLDG 32235 ELMENDORF AFB AK 99506-3097	1
DET 1 3 ASOS/GEW BLDG 1558 FT WAINWRIGHT AK 99703-5200	1
607 WEATHER SQUADRON/DO UNIT 15173 BLDG 1506 APO AP 96205-0108	2
611 OSS/OSW 6900 9TH ST STE 205 ELMENDORF AFB AK 99506-2250	1
C/O FT RICHARDSON NCOIC 611 OSS/WE 6900 9TH ST STE 205 ELMENDORF AFB AK 99508-2250	1
354 OSS IM 1215 FLIGHT LINE AVE STE 2 EIELSON AFB AK 99702-1520	1
ARMED FORCES MEDICAL INTELLIGENCE CTR INFO SVCS DIV BLDG 1607 FT DETRICK FREDERICK MD 21702-5004	1
ARMY TRAINING AND DOCTRINE COMMAND ATDO-IW (ATTN: SWO) FT MONROE VA 23651-5000	1
ARMY RESEARCH LABORATORY BATTLEFIELD ENVIRONMENT DIR AMSRL-BE WHITE SANDS MISSILE RANGE NM 88002-5501	1
USASOC ATTN: AOIN-ST FT BRAGG NC 28307-5200	1
ARMY COMBAT SYS TEST ACTIVITY MET BRANCH, BLDG 1134 ATTN: STECS-PO-OM ABERDEEN PRVNG GRND MD 21005-5059	1
COMMANDER US ARMY PACIFIC (APIN-OPW) FT SHAFTER HI 96858-5100	1
COMMANDER, FORCES COMMAND AFIN-ICW FT MCPHERSON GA 30330-6000	1
DIRECTOR USA-CETEC ATTN: GL-AE FT BELVOIR VA 22060-5546	1
DIRECTOR, USA REDSTONE TECHNICAL TEST CENTER ATTN: STERT-TE-F-MT REDSTONE ARSENAL AL 35898-8052	1
FIRST US ARMY ATTN STAFF WEATHER OFFICER FT MEADE MD 20755-7300	1
SECOND US ARMY AFKD-OPI-W (AFDIS POC) FT GILLEM GA 30050-5000	1
HQ DA DCS OPERATIONS AND PLANS ATTN: DAMO-ZD RM 3A538, 400 ARMY PENTAGON WASHINGTON DC 20330-5000	1
HQ 629TH MI BN (CEWI), 29TH ID (LIGHT) 7100 GREENBELT ROAD GREENBELT MD 20770-3398	1
FIFTH U.S. ARMY AFKB-OP (SWO) FT SAM HOUSTON TX 78234-7001	1
SIXTH US ARMY AFKC-OP-IS-SWO (AFDIS POC) PRESIDIO SAN FRANCISCO CA 94129-5000	1
HQ ARCENT AFRD-DSO-SWO FT MCPHERSON GA 30330-7000	1
LOS ALAMITOS AAF (MR ADAMS) BLDG 1 AFRC 11200 LEXINGTON DR LOS ALAMITOS CA 90720-5001	1
NATIONAL RANGE DIRECTORATE MET BRANCH ATTN: STEWS-NR-DA-F WHITE SANDS MISSILE RANGE NM 88002-5504	1
TECHNICAL LIBRARY DUGWAY PROVING GROUND DUGWAY UT 84022-5000	1
TEXCOM FSTD ATTN: CSTE-TFS-SP FT SILL OK 73503-6100	1
USA TECOM ATTN: AMSEL-TC-AM(BE) C O NVESD FT BELVOIR VA 22060-5677	1
USA INTELLIGENCE CTR (WEATHER SUPPORT TEAM) ATTN ATZS CDI-W FT HUACHUCA AI AZ 85613-6000	1
USA DUGWAY PROVING GROUND TROPICAL TEST SITE UNIT 7140 ATTN: STEDP-MT-TM-TP APO AA 34004-5000	1
USA TECOM ATTN: AMSEL-RD-NV-VMD (MET) FT BELVOIR VA 22060-5677	1
USA ARMY ENGINEER TOPOGRAPHIC LAB ATTN: CEETL-TD FT BELVOIR VA 22310-3864	1
USARSPACE (MOSC-OO) 1670 N NEWPORT RD STE 121 COLORADO SPRINGS CO 80916-2749	1
1CC AZSB-GTFD AH-64 CSM ATTACK FT CAMPBELL AI KY 42223-5000	1
160TH SOAR(A) ATTN: ADAV-ST-FS(MR LEVARN) 6950 38TH STREET FT CAMPBELL KY 42223-1291	1
OL A AFCOS FT RICHIE MD 21719-5010	1
AFESC/RDXT BLDG 1120 STOP 21 TYNDALL AFB FL 32403-5000	1
AFOSR/NL BOLLING AFB DC 20332-5000	1
AFRES/DOTSC 155 2ND ST ROBINS AFB GA 31098-1635	1
AFTAC 1030 SOUTH HIGHWAY A1A PATRICK AFB FL 32925-3002	1
ANGRC/DOSW 3500 FETCHET AVENUE ANDREWS AFB MD 20331-5157	1
DET 3 DOWX 1900 WEST FLAMINGO STE 266 PO BOX 19070 LAS VEGAS NV 89119-5116	1
USAF DFEG FAIRCHILD HALL USAF ACADEMY CO 80840-5701	1

USFA DEPT OF ECONOMICS & GEOGRAPHY COLORADO SPRINGS CO 80840-5701	1
HQ JTF-PP (LT STEADLY/USN) APO AE 09784-5000	1
NATO IMS (OPS DIVISION) PSC 80 BOX 36 APO AE 09724-5000	1
NATO LMS/OPS STAFF METEOROLOGICAL OFFICER APO AE 09724	1
AFSOUTH (CMFWC CAPT STRAYER) PSC 813 BOX 136 FPO AE 09620-5000	1
USAFE XOOWUNIT 3050 BOX 15 BLDG 546 ROOM 306 APO AE 09094-5015	1
3 AF/DOW UNIT 4840 APO AE 09459-4840	1
5 ATAF WEA OFFICE 5 ATAF WEATHER CENTRE 36100 VINCENZA ITALY	1
10 OSS OSW UNIT 5605 BOX 175 APO AE 09470-5175	1
16 AF WE UNIT 6365 APO AE 09601-6365	1
17 AF/WE UNIT 4065 APO AE 09136-5000	1
617 WS UNIT 29351 BLDG 12 APO AE 09014-5000	4
COMNAVMETOCCOM STENNIS SPACE CTR MS 39529-5000	1
COMNAVSPCWARCOM (CODE N27 FORCE OCEANOGRAPHER) 2000 TRIDENT WAY SAN DIEGO CA 92155-5599	1
COMSECONDFLEET (CODE J335) FPO AE 09506-6000	1
COMSIXFLEET (CODE N312) CDR MCGEE FPO AE 09501-6002	1
FLENUMMETOCEN ATTN: DAVE HUFF MONTEREY CA 93943-5005	1
FLENUMMETOCDET FEDERAL BUILDING ASHEVILLE NC 28801-2696	1
LIBRARIAN FLENUMMETOCEN MONTEREY CA 93943-5005	1
HQ USMC (CODE ASL-44/MAJOR BROWN) 2 NAVY ANNEX WASHINGTON DC 20380-1775	1
MARINE WING SUPPORT GROUP 27 (WO) PSC BOX 8082 CHERRY POINT MCAS NC 28532-8082	2
NAVAL RESEARCH LABORATORY MONTEREY CA 93943-5006	1
NAVAL RESEARCH LABORATORY CODE 4180 WASHINGTON DC 20375	1
NAVAL RESEARCH LABORATORY CODE 4323 WASHINGTON DC 20375	1
NAVAL POSTGRADUATE SCHOOL CODE MR/HY (ROBERT HANEY) 589 DYER RD BLDG 235 RM 2AF MONTEREY CA 93943-5114	1
NAVAL POSTGRADUATE SCHOOL CHMN DEPT OF METEOROLOGY CODE 63 MONTEREY CA 93943-5000	1
NAVAL AIR WARFARE CENTER-WEAPONS DIVISION GEOPHYSICAL SCIENCES BRANCH CODE 32AF POINT MUGU CA 93042-5001	1
COMMANDING OFFICER NAVEURMETOCEN PSC 819 BOX 31 FPO AE 09645-3200	1
OFFICER IN CHARGE NAVEURMETOCDET PSC 817 BOX 13 FPO AE 09622-0800	1
OFFICER IN CHARGE NAVEURMETOCDET PSC 814 BOX 22 FPO AE 09865	1
OFFICER IN CHARGE NAVEURMETOCDET PSC 812 BOX 3380 FPO AE 09627-3380	1
NAVICEEN (LT KLEIN) 4251 SUITLAND RD FOB#4 WASHINGTON DC 20395	1
COMMANDING OFFICER NAVICEEN 4301 SUITLAND ROAD FOB #4 WASHINGTON DC 20395-5108	1
NAVLANTMETOCDET PATUXENT RIVER NAS MD 20670-5103	1
NAVLANTMETOCDET (AFDIS POC) PSC 1001 BOX 35-W FPO AE 09508-0014	1
NAVLANTMETOCEN 931 3 RD AVE MCCADY BLDG NORFOLK NAS VA 23511-2394	1
NAVLANTMETOCEN CODE 50, ATTN: MET TEAM 931 3RD AVE MCCADY BLDG NORFOLK NAS VA 23511-2394	1
NAVOCEANO CODE N2513 1002 BALCH BLVD STENNIS SPACE CTR MS 39522-5001	1
MAURY OCEANOGRAPHIC LIBRARY NAVOCEANO N4312 BLDG 1003 STENNIS SPACE CTR MS 39522-5001	1
OCEANOGRAPHER OF THE NAVY (AGCS KAEMPFER) US NAVAL OBSERVATORY BLDG 1 3450 MASS AVE WASHINGTON DC 20392-5421	1
HQ USMC (CODE ASL-44) 2 NAVY ANNEX WASHINGTON DC 20380-1775	1
AEDC TECHNICAL LIBRARY FL2804 100 KINDEL DR STE C212 ARNOLD AFB TN 37389-3212	1
HUMAN RESOURCES TECHNICAL LIBRARY FL2870 AL/HR-DOKL 7909 LINDBERG DR RM 239 BLDG 578 BROOKS AFB TX 78235-5352	1
AFMTC TECHNICAL LIBRARY FL2806 412 TW/TSTL 307 E POPSON AVE BLDG 1400 RM 106 EDWARDS AFB CA 93524-6630	1
TECHNICAL LIBRARY FL2825 203 W EGLIN BLVD STE 300 EGLIN AFB FL 32542-6843	1
ROME LAB TECHNICAL LIBRARY FL2810 RL/SUL CORRIDOR W STE 262 26 ELECTRONIC PKWY BLDG 106 GRIFFISS AFB NY 13441-4514	1
ROME LAB RESEARCH LIBRARY FL2807 PL/TL (LIBRARY) 5 WRIGHT ST BLDG 1103 HANSCOM AFB MA 01731-3004	1
TECHNICAL LIBRARY FL2051 SA-ALC/CNL 485 QUENTIN ROOSEVELT RD BLDG 171 KELLY AFB TX 782416425	1
PHILIPS LAB TECHNICAL LIBRARY FL2809 PL/DOSUL 3400 ABERDEEN AVE SE BLDG 419 KIRTLAND AFB NM 87117-5776	1
AIR UNIVERSITY LIBRARY FL3386 AUL/LD 600 CHENNAULT CIRCLE BLDG 1405 MAXWELL AFB AL 36112-6424	1
AUL/LSE BLDG 1405 600 CHENNAULT CIRCLE MAXWELL AFB AL 36112-6424	1
TECHNICAL LIBRARY FL3100 HQ SSC/RMMI 201 E MOORE DR BLDG 856 RM 1701 MAXWELL AFB GUNTER ANNEX AL 36114-3005	1
TECHNICAL LIBRARY FL2513 45 SW CSR 5123 1030 S HWY A1A BLDG 989 RM A1-S3 BOX 4127 PATRICK AFB FL 32925-0127	1
TECHNICAL INFO CTR FL7050 AL/EQ-TIC 139 BARNES DR STE 2 BLDG 1120 TYNDALL AFB FL 32403-5323	1
TECHNICAL LIBRARY FL2827 30 SPW/XPOT 806 13TH ST STE A BLDG 7015 VANDENBERG AFB CA 93437-61111	1
WRIGHT LAB LIBRARY FL2802 WL/DOC 2690 C ST STE 4 BLDG 22 WRIGHT-PATTERSON AFB OH 45433-7411	1
TECHNICAL LIBRARY FL2830 NAIC/DXLS AREA A 415 HEBBLE CREEK RD STE 9 BLDG 85 WRIGHT-PATTERSON AFB OH 45433-6508	1

USAF LIBRARY FL7000 HQ USAFA/DFSEL 2354 FAIRCHILD DR STE 3A10 USAF ACADEMY CO 80840-6214	1
DEFENSE INTELLIGENCE AGENCY DIA D1W 1B DIAC RM A4-130 WASHINGTON DC 20340-6612	1
DTIC-FDAC CAMERON STATION ALEXANDRIA VA 22304-6145	3
NASA-MSFC HUNTSVILLE AL 35812-5000	1
NASA GODDARD MAIL CODE 916 GREENBELT MD 20771	1
OFMC FEDERAL COORDINATOR FOR METEOROLOGY 8455 COLESVILLE ROAD STE 1500 SILVER SPRING MD 20910-5000	1